Simulation of Transport Phenomena in Fractured Rocks with Application to Hot-Dry-Rock Geothermal Systems

Sergei Fomin*, Zhenzi Jing and Toshiyuki Hashida

Fracture and Reliability Research Institute, Tohoku University, Sendai 980-8579, Japan
*E-mail: fomin@rift.mech.tohoku.ac.jp

The numerical model FRACSIM-3D developed by a research group at Tohoku University for the hot-dry-rock (HDR) geothermal reservoir has proven to be an appropriate approximate model capable of simultaneously addressing problems associated with hydraulic stimulation, fluid circulation, and heat extraction. The models of fracture networks are generated by distributing fractures randomly in space and considering the fractal correlation. Based on this approach, a mathematical model of the mechanical water-rock interaction, which accounts for variations of permeability due to fracture opening subsequent upon injection pressure increase, is proposed. The model incorporates approximations of the fracture mechanical behavior drawn from the rock mechanics literature, a very simplified analysis of the operative physical processes, and mapping of the connectivity of fracture network to a cubic regular grid. The water/rock chemical interaction (WRCI) is the other factor that inevitably exerts an influence on the permeability of the high temperature deep HDR circulating system. In the present study an improved mathematical model, which accounts for the effects of thermal dispersion and WRCI (in terms rock chemical dissolution and precipitation), is proposed. The numerical analysis based on the 3D model of the reacting fluid flow within the fractured media proves the importance of the thermal dispersion and WRCI factors for the assessment of the overall reservoir thermal and hydraulic performance.

1. Introduction

Many numerical models have been proposed for simulating the HDR systems [1-3]. The numerical model FRACSIM-3D developed by the research group in Tohoku University is proved to be an appropriate approximate model capable to address simultaneously the problems associated with hydraulic stimulation, fluid circulation and heat extraction and can quantitatively predict the 3D reservoir growth behaviour. In fractured rocks, groundwater flow occurs predominantly through the connected network of discrete fractures. A series of geophysical investigations has confirmed that subsurface fracture networks can commonly be described by fractal geometry. The model presented here is based on the relationship between the fracture length and a number of fractures, as suggested in Watanabe & Takahashi [2]. It incorporates the elements of the approximate model discussed in Jing et al. [3], where the fracture shear displacements and openings, variation of the shape of the stimulating rock volume, pressure compliant fracture apertures are taken into account. Since the fluid velocity within the geothermal reservoirs created in the fractured rock can be relatively high and the characteristic sizes of the solid blocks of the rock, which constitute the fissured reservoir media, are relatively large, the high mean values of heat flow rates are typically attained within the stimulated region. In this situation the effect of thermal dispersion is an important factor, which is included into the mathematical model of the heat transport within the natural or artificially developed fissured geothermal reservoirs. Mathematical model also accounts for the effects of rock chemical dissolution and precipitation.

2. Mathematical Model

In the present 3D model the fracture network, which consists of the randomly distributed penny-shaped subsurface fractures, is mapped on a regular cubical grid of the discretized reservoir domain. It is assumed that the flow properties of a stochastic fracture network depend on the fluid pressure. Fractures are generated stochastically within a fracture generation volume of $(L+2r_{max})^3$, where L

is the characteristic linear dimension of the model volume and r_{max} is the radius of the largest fracture. The fracture centers are uniformly-randomly distributed. In 3D case the radius of the penny-shaped fracture is used as a characteristic fracture dimension (instead of fracture length in 2D-model) and will be quoted as a fractal fracture length in the further discussion. The random fractures are generated as follows. In a fractal fracture length distribution of fractal dimension D, the number of fractures N_r whose characteristic length (in terms of fracture radius r) is greater than r, is given by $N_r=Br^{-D}$, where B is fracture density within the rock mass. Hence, the number of fractures between the specified upper and lower limits is given by $N_{r_{min}}^{r_{max}} = B(r_{min}^{-D} - r_{max}^{-D})$, where r_{min} and r_{max} are the lower and upper fracture radius limits, respectively. Consider some fraction, α, of this total number counting from r_{min} upward and the corresponding size r_α of the largest object in that fraction, then $N_{r_{min}}^{r_\alpha} = \alpha B(r_{min}^{-D} - r_{max}^{-D}) = B(r_{min}^{-D} - r_\alpha^{-D})$. The latter yields the fractal fracture length distribution

$$r_\alpha = [(1-\alpha) r_{min}^{-D} + \alpha r_{max}^{-D}]^{-1/D}, \qquad (1)$$

where α is a random parameter in the interval [0,1]. Thus, for the purpose of simulation, it is necessary to specify the length of the smallest and largest fractures, as well as fractal dimension D. Using equation (1), fracture r_α can be generated by simply changing the α value. For any generated fracture, the initial (i.e. undisturbed) fracture aperture, a_0, when evaluated at zero effective stress, is assumed to be proportional to the fracture radius, $a_{i0} = \beta \cdot r_i$, where i=1, 2,…, N_f and r_i is the radius of each fracture from the whole set of fractures N_f; β is a constant of proportionality, which is chosen to allow the undisturbed fracture network to match (at least approximately) the *in situ* measured permeability. Fracture orientation distribution is based on the fracture orientations that obtained (usually from well logs) by field observations at the HDR geothermal reservoir. Fractures are generated until the fracture density (total area of fracture surfaces per rock volume) reaches the experimentally observed level.

2.1. Reservoir dynamics Fracture apertures are affected by the effective normal stress at the fracture surface and by shear displacement that determines the fit of the opposing rough surfaces. Shear stability is expressed by a simple friction law, when slip is taking place if $\tau > (\sigma_n - P)\tan(\phi_i + \phi_{dil}^{eff})$, where τ is a shear stress, σ_n is the rock stress normal to the fracture surface, P is a fluid pressure in fracture, and ϕ_{dil}^{eff} is an effective shear dilation angle at a given effective normal stress. The basic friction angle ϕ_i is a material property of the fracture walls. The effective shear dilation angle ϕ_{dil}^{eff} is a property of both the fracture wall asperities and effective normal stress

$$\tan(\phi_{dil}^{eff}) = \tan(\phi_{dil}) / [1 + 9(\sigma_n - P)/\sigma_{nref}], \qquad (2)$$

where σ_{nref} is the effective normal stress applied to cause a 90% reduction in the compliant aperture and ϕ_{dil} is the laboratory measured shear dilation angle at very low effective stress. The amount of shear displacement depends on the fracture shear stiffness and on the amount of "excess" shear stress available. Referring to the theory of elasticity, the shear displacement of a fracture U can be expressed as:

$$U = [\tau - (\sigma_n - P)\tan(\phi_i + \phi_{dil}^{eff})] / H_s, \qquad (3)$$

where H_s is a shear stiffness of the fracture. The change in aperture is a product of the displacement and the tangent of the effective shear dilation angle $a_s = U\tan(\phi_{dil}^{eff})$. An expression for the aperture a of a sheared fracture with unabrading asperities in contact is

$$a = (a_0 + U\tan(\phi_{dil})) / [1 + 9(\sigma_n - P)/\sigma_{nref}]. \qquad (4)$$

The above equations provide a simple set of approximate correlations used in a model that contains many thousands of fractures each of which might undergo a small displacement. Since the flow rate in the reservoir is relatively high (especially during reservoir hydraulic stimulation) and, therefore, form drag due to solid obstacles may be comparable with the surface drag due to friction. Moreover, in some numerical models, for instance the 3D Finite Element Program FRACTure [1], the terms that govern the surface drag is ignored initially, referring to the fact of high flow rate, and only Forchheimer drag is incorporated. To this end, it would be quite useful to obtain the reliable estimates (at least to the order of magnitude) of the forces acting in the fractured media and validate the model for momentum equation before proceeding with complex numerical simulations. This can be

made on the basis of scale analysis of the momentum equation that accounts for the both effects mentioned above. This equation can be presented as:

$$\nabla P = -\frac{\mu q}{2\pi K r_w h_w}(\tilde{\mathbf{u}} + c_F \,\mathrm{Re}|\tilde{\mathbf{u}}|\tilde{\mathbf{u}}), \qquad (5)$$

where $c_F \approx 0.55$ is a dimensionless form-drag (Forchheimer) constant, q is a flow rate in the borehole, $\tilde{\mathbf{u}} = \mathbf{u}/u_0$ is a non-dimensional value of filtration velocity vector $\mathbf{u}(u_x, u_y, u_z)$ which is scaled with $u_0 = q/(2\pi r_w h_w)$, $\mathrm{Re} = \sqrt{K} u_0 \rho_L / \mu$ is Reynolds number, r_w is borehole radius, h_w is characteristic vertical sizes of the model area; K permeability of the media, μ and ρ_L fluid viscosity and density, respectively. For the typical conditions of the geothermal reservoir exploitation, h_w=100m, ρ_L=1000kg/m^3, q=200·10^{-3}m^3/s, μ=3·10^{-4}s·N/m^2, r_w=0.1m and K=10^{-14}m^2, we have Re≈10^{-3}. Hence, flow is laminar and the Forchheimer drag force can be neglected in the model. In this case the linear Darcy momentum equations can be employed, namely,

$$u_f = -(K_f/\mu)(\partial P/\partial f), \qquad (6)$$

where f=x, y, z. At this point it should be noted that in FRACSIM model the fractured reservoir is considered as an orthotropic media with symmetric permeability tensor and a diagonal matrix is formed whenever the coordinate axes are parallel with the principal axes along which the coordinates of the permeability tensor are K_x, K_y, K_z. Accounting for the mass conservation equation, the Darcy flow model leads to the following equation for pressure distribution

$$\frac{\partial}{\partial x}\left(K_x \frac{\partial P}{\partial x}\right) + \frac{\partial}{\partial y}\left(K_y \frac{\partial P}{\partial y}\right) + \frac{\partial}{\partial z}\left(K_z \frac{\partial P}{\partial z}\right) = 0. \qquad (7)$$

The permeability in the x, y and z directions, is strongly affected by the fracture distribution and fracture dimensions. Since the fracture apertures depend on pressure in the fluid and normal and shear stresses (see equations (3) and (4)), the permeability of the reservoir (defined by its components K_x, K_y, K_z), should be treated as a functions of spatial coordinates (x, y, z) and pressure P. As a result the problem is formulated as strongly non-linear, with variable permeability and, therefore, numerically it can be solved only by iterations.

2.2. Heat and mass transfer processes. Since the fluid velocity within the geothermal reservoirs created in the fractured rock can be relatively high and the characteristic sizes of the solid blocks of the rock, which constitute the fissured reservoir media, are relatively large, the high mean values of heat flow rates are typically attained within the stimulated region. In this situation the effect of thermal dispersion is an important factor that should be included into the mathematical model of the heat transport within the natural or artificially developed fissured geothermal reservoirs. Employing different theoretical methods such as, volume averaging, moment-matching, homogenisation, moment-difference expansion, and others [4,5], and also experimental approaches it was proved that the approximate macro-scale model of heat transport within the fractured media in whole provides a quite sufficient level of accuracy and can be readily used instead of the exact model on the micro-scale level. The length L, which characterizes the whole volume of the fractured media, is assumed to be significantly larger than the spatial representative scale l for the unit cell (solid block), so that the small parameter can be introduced as $\varepsilon = l/L << 1$. For convenience, further we will assume that z-axis of the Cartesian coordinates coincides with the axis of symmetry of the borehole and the dominant flow in the reservoir is orthogonal to z- axis. In the publications cited above it was rigorously proved that with the accuracy of $O(\varepsilon)$ the macro-scale temperature equation for this flow can be formulated as:

$$c\rho \frac{\partial T}{\partial t} + c_L \rho_L \mathbf{u} \cdot \nabla T = \\ = \frac{\partial}{\partial x}\left(k_{\parallel} \frac{\partial T}{\partial x}\right) + \frac{\partial}{\partial y}\left(k_{\parallel} \frac{\partial T}{\partial y}\right) + \frac{\partial}{\partial z}\left(k_{\perp} \frac{\partial T}{\partial z}\right), \qquad (8)$$

where c=$c_L m$+$c_S(1-m)$, ρ=$\rho_L m$+$\rho_S(1-m)$ are effective specific heat and effective density, respectively; indexes L and S indicate liquid and solid phase; m is porosity; t is time; $k_{\parallel}$ and $k_{\perp}$ are the longitudinal (parallel to the dominant flow) and the orthogonal (transverse to the main flow) effective thermal conductivities that account for the stagnant effective conductivity k and thermal dispersion which occurs due to hydrodynamic mixing of the interstitial fluid at the solid block scale. The effect of thermal dispersion, results in the apparent increase of thermal conductivity of the porous media. It is well documented that $k_{\parallel}, k_{\perp}$

depend on the fluid velocity and geometry of the media. For the relatively high velocities, (typical Peclet numbers: $Pe=u_0 l/d_s \sim 10^2$ - 10^3, where d_s is thermal diffusivity of the rocks) the components of effective conductivity tensor for the fractured and porous media of different structure and geometry can be presented as

$$k_{\parallel} = k + A(c_L \rho_L |\mathbf{u}| l)^{\gamma}, \quad k_{\perp} = k + B(c_L \rho_L |\mathbf{u}| l), \qquad (9)$$

where $k=k_L m+k_S(1-m)$ is stagnant effective thermal conductivity, $|\mathbf{u}| = (u_x^2 + u_y^2 + u_z^2)^{1/2}$, parameters B, A and γ depend on the geometry of the fracture, fracture distribution and physical situation. For instance, if the medium is such that mixing effect dominates, then $\gamma=2$. For the medium where dispersion takes place mostly owing to the velocity variation inside the network [5], which apparently is our case, $\gamma=1$. The above equations with the corresponding boundary conditions constitute the basic mathematical description of the heat transport in the geothermal reservoir. Operation of the HDR geothermal system is expected to proceed for a long time. Water/rock chemical interaction inevitable exerts an influence on the permeability of these high temperature and pressure circulating systems due to dissolution and deposition processes. The model for the water/rock chemical interaction adopted in FRACSIM numerical code is based on a set of simple equations proposed and discussed in detail by Jing et al [6]. Variation of dissolved rock concentration C and fracture aperture a are described by the following equations

$$\frac{\partial C}{\partial t} + \mathbf{u} \cdot \nabla C = \\ = \frac{\partial}{\partial x}\left(D_{\parallel} \frac{\partial C}{\partial x} \right) + \frac{\partial}{\partial y}\left(D_{\parallel} \frac{\partial C}{\partial y} \right) + \frac{\partial}{\partial z}\left(D_{\perp} \frac{\partial C}{\partial z} \right) \qquad (10)$$

$$\frac{\partial a}{\partial t} = R(T)[C_{\infty}(T(x,y,z,t)) - C(x,y,z,t)], \qquad (11)$$

where $R(T)$ and $C_{\infty}(T)$ are the temperature-dependent reaction rate and the saturation concentration; $D_{\parallel}$ and $D_{\perp}$ are the longitudinal (parallel to the dominant flow) and the orthogonal (transverse to the main flow) effective dispersion coefficients that account for the stagnant diffusivity and mechanical dispersion due to hydrodynamic mixing of the interstitial fluid. These equations, coupled with temperature equation, are used for simulating the fracture aperture variation due to dissolution/deposition within the reservoir fracture network during the production stage of the reservoir exploitation.

2.3. Numerical algorithm The numerical simulation of the fractured reservoir behaviour can be decomposed into two main parts. Namely, hydraulic fracturing part (here at first the values of the fracture shear dilation angles should be obtained for the typical rock in reservoir), and, after that, the model of the stimulated reservoir is employed for evaluating the heat and mass transfer processes during the production stage of reservoir exploitation. Initially, a 3D stochastic network of many thousands of fractures (which length satisfy equation (1)) is generated within a cubic domain $L \times L \times L$. Equations that govern the reservoir dynamics and heat and mass transfer processes in the fractured media are solved numerically by the finite difference method, when the computational domain is composed from $l \times l \times l$ of square grid elements (blocks) which typical scale $l<<L$, as discussed in Jing et al. [6]. For each block, some fractures will intersect with its faces. It is assumed that each intersecting fracture has width l_j, aperture a_j and length l (equal to block length). The fracture network is assumed to be well connected. The quantity of a fluid flow from block to block is controlled by Darcy law with the permeability contribution from each fracture governed by the sum of the products of the fracture apertures to the 3rd power and length of the intersection of the fracture with the block face. Summing the contribution of each fracture, the effective permeability connecting the blocks of the grid is used to perform the flow computations. The present model uses the vertical stress and two horizontal principal stresses, which are taken to be the maximum and minimum principal stresses. In order to predict the maximum reservoir size, the present stimulation code calculates the flow rate and pressure distribution during stimulation within the field; afterwards the fracture shear displacements are obtained. The discretized steady-state flow equation (7) is solved by the Gauss-Seidel method. The numerical algorithm accounts iteratively for the fluid flow that affects the fracture aperture and pressure distribution. The changes in pressure and fracture aperture induce a shear displacement that consequently leads to a new change in pressure distribution. Provided the spatial distribution of permeability is given, the pressure is calculated by iteration; the aperture value responds to the deviation of the local pressures according to equations (3) and (4). The latter yields the change

of transmissibility of the rock. Then a new calculation (equation (7)) for the pressure distribution is required. These steps are repeated until the flow rate and the transmissibility converge. Using this method, the maximum reservoir size is determined. After the fluid velocities are determined, equation (8) for the temperature field within the reservoir is solved numerically by the Alternative Direction Implicit method while the constant temperature boundary conditions are assumed. On the next step of reservoir numerical simulation at production stage, variation of the fracture apertures due to chemical dissolution/precipitation is calculated (equations (10),(11)). The latter affects the permeability of the rock. For the changed permeability, new calculations for the pressure and temperature distributions are required. Hence, similarly to the stimulation part, at this stage the iterative algorithm is employed.

3. Results and conclusions

Computations performed for the stimulating stage of the reservoir exploitation provide the new data for the stimulated area, namely, the size of the stimulated volume, the number of the stimulated fractures and their new apertures. For the heat extraction stage the pressure in the injection well is assumed equal to 0.5 MPa and 0 at the production well. As a result the injection flow rate is computed as 1.52 10^{-2} m^3/sec and production flow rate is 1.14 10^{-2} m^3/sec. The recovery rate of the reservoir is estimated as 75%, which is in a good consistency with Hijiory field measurements. The influence of the dispersion effect on the heat flow within the reservoir is illustrated in Fig. 1. The curves in this figure correspond to the temperatures in the production well computed for different effective heat conductivities. The solid line in Fig. 1 illustrates to the time variation of the temperature in the production well when the effect of thermal dispersion is ignored. As it can be seen the temperature in the output can be in some cases about 20% percent higher when thermal dispersion takes place (see the case when A=0.1, B=1). For the smaller values of A and B (A=0.1, B=0.5 or A=0.05, B=1) the effect of thermal dispersion is less profound. For the higher injection well pressure the flow rate increases which consequently leads to the increase of the effective thermal conductivity. For instance for the higher injection pressure up to 1 MPa the effect of thermal dispersion leads to the 10% rise of the temperature in the production well. Although the input data for calculations are specified for the Hijiori reservoir conditions the general conclusion can be drawn. Namely, ignoring the effect of heat dispersion may lead to a significant underestimation of the total amount of heat extracted during its production period.

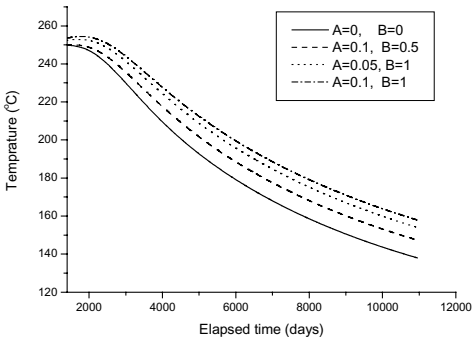

Fig. 1. The computed temperature in the production well for different effective thermal conductivities defined by equations (9).

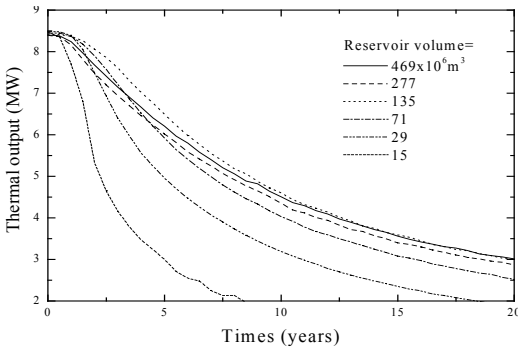

Fig. 2. Variation of the thermal output *vs* time; the recovery rate=20*l/sec*.

Series of computations carried out for the reservoirs of different volumes indicates that the size of the reservoir is a crucial factor for its productivity. The related results are presented in Fig. 2. As it can be seen, the size of the reservoir has a significant influence on the value of the thermal output. It is worthwhile mentioning that the stimulated volume of the reservoir is determined during the first, stimulation stage of the reservoir exploitation. Therefore, the assessment of the reservoir productivity should include all the factors that may affect the value of the reservoir thermal output. In mathematical terms the adequate mathematical

model should account for the fracture dilation during the stimulation stage and thermal dispersion during the production period.

The 3-D WRCI model has been used to examine the effects of WRCI on the long-term performance of the HDR system. In equation (11) parameters $R(T)$ and $C_{\infty}(T)$ depend on temperature. Therefore, the initial rock temperature may affect the WRCI within the reservoir. The initial rock temperatures are assumed to be equal to 150, 200, 250 and 300 ^{o}C. The effect of these temperatures on the flow rate at injection pressure of 8 MPa is shown in Fig. 3.

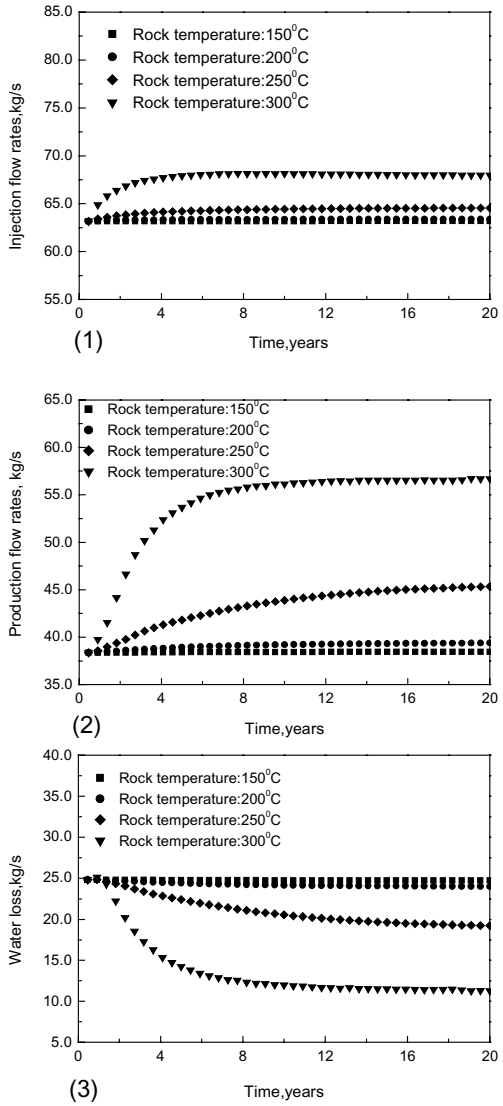

Fig. 3. Effect of initial rock temperature on flow rates and water loss due to the influence of WRCI. The higher the temperature, the greater the effect.

The greater injection and production flow rates are observed for higher initial rock temperature, which indicates the sensitivity of WRCI to the initial temperatures. The flow rate remains almost the same when the initial rock temperature is relatively law - up to 150^{o}C. It can be attributed to the fact that at these temperatures WRCI is less intensive and this practically does not affect the reservoir permeability. Whereas, at higher initial rock temperatures the WRCI increases and this may lead to rather significant variation of the flow rate. Hence, for the hotter (or deeper) reservoir the effect of WRCI can be very pronounced. For the rock temperatures of 300^{o}C (which is close to supercritical stage) there is a rapid increase in production flow rate (see Fig. 3(2)), which takes place over the first 6 years. In contrast, more gradual increase in production flow rate can be observed for the same time period in the rocks at 250^{o}C. Since at initial stage of reservoir exploitation temperatures are very high, the solvability of the rocks is also respectively higher. The latter results in a sharp increase of permeability, which in term enhance the flow rate.

Acknowledgements

The work was partially supported by the Grants-in-Aid for Scientific Research (A) (No. 14205149) and (C) (15560130), The Japan Society for the Promotion of Science and by the 21st Century COE Program Grant of the International COE of Flow Dynamics from the Ministry of Education, Culture, Sports, Science and Technology.

References

[1] T. Kohl & R.J. Hopkirk, *Geothermics* , **24(3),** 333 (1995).

[2] K. Watanabe and T. Takahashi, *Journal of Geophysical Research,* **100(B1),** 521 (1995).

[3] Z. Jing, J. Willis-Richards, K. Watanabe & T. Hashida, *Journal of Geophysical Research*, **105(B10)**, 23663 (2000).

[4] C.T. Hsu, & P. Cheng, *Journal of Heat and Mass Transfer,* **33,** 1587 (1990).

[5] J. Koplik, S. Redner and D. Wilkinson, *Physical Review A,* **37,** 2619 (1988).

[6] Zh. Jing, K. Watanabe, J. Willis-Richards, & T. Hashida, *Geothermics*, **31**, 1 (2002).